Spectra of liquid helium and hydrogen-doped liquid helium

A. Trottier, A. I. Jirasek, H. F. Tiedje, and R. L. Brooks
Guelph-Waterloo Physics Institute, University of Guelph, Guelph, Ontario, Canada N1G 2W1
(Received 12 November 1999; published 7 April 2000)

Proton-beam irradiation, using the 3 MV accelerator at Guelph, has been successful in allowing us to study the emission spectra from liquid helium and hydrogen-doped liquid helium despite the fact that the beam penetrates the target a scant 0.5 mm. H_2 emission lines can be observed from liquid samples following doping with small amounts of hydrogen into the helium gas before condensation. The line intensities are a sensitive function of the sample temperature, becoming strongest as the liquid approaches 4.2 K. The H_2 lines themselves are much broader than those from He_2 because the helium lines actually originate in small bubbles of helium gas trapped in the liquid, which is above the λ point. The interesting fact is that electronic emission spectra from H_2 are observed at all from liquid helium and a calculation of the widths and shifts of the spectral lines will be presented.

PACS number(s): 33.70.Jg, 67.20.+k, 78.60.−b

I. INTRODUCTION

The use of liquid helium as a possible matrix for performing spectroscopy on atoms and molecules in a cryogenic environment is receiving renewed interest with the use of evaporatively cooled helium droplets as the environment [1]. However, studies using bulk liquid helium, both as a comparison for the droplet measurements and as a medium with controlled temperature and pressure, are still desirable.

Using proton-beam irradiation, from a 3 MV Van de Graaff accelerator at the University of Guelph, we can achieve about 500 μm penetration of a bulk liquid helium target, which is sufficient for us to spectroscopically examine the light emitted at right angles to the proton beam using either a Bomem FTIR spectrometer or a 0.3 m McPherson grating spectrometer. Similar measurements using solid hydrogen targets, gaseous helium targets, or combinations of the two [2] have been performed by us for a number of years mostly at the now defunct McMaster University Tandem Accelerator. One technique, developed by us, was to put cold helium gas above a thin film of solid hydrogen, which upon irradiation, produced emission whose spectra revealed the presence of helium hydride excimers [3,4]. By extending that idea to having liquid helium above a thin film of solid hydrogen, we were able to identify molecular hydrogen emission spectra, which are the subject of this report. No helium hydride was observed.

In 1968 Surko and Reif [5] found that a radioactive source immersed in liquid helium could create neutral localized excitations. Fischbach *et al.* [6] found evidence for long lived excitations in liquid helium both above and below the λ point [7]. These excitations produced emissions that were tentatively attributed to metastable states.

To clarify the situation, Dennis *et al.* [8] performed an experiment in superfluid helium using electron bombardment as the excitation method. His group was able to identify several features arising from electronically excited states of He_2. Both singlet and triplet states were found to be populated, including the metastable $a\,^3\Sigma_u^+$ state. In addition they found that metastable $2s\,^3S_1$ helium atoms were created by the excitation processes. While all features were both broadened and shifted from the corresponding gas phase spectra, this effect was smaller than anticipated.

These studies led to the idea of helium ''bubbles'' arising from the repulsion between the helium molecule and the ground-state atoms of the liquid. This is similar in nature to an electron bubble observed in related experiments, where it is a free electron that forms the bubble [9–12]. A more recent paper shows that a bubble can also be formed by an excited barium atom placed in liquid helium [13]. Laser ablation experiments have studied excited states of mostly alkali and alkali-earth atoms, dimers, and clusters in liquid helium both above and below the λ point [14,15]. A recent review examines these experiments and others that have implanted impurities in superfluid liquid ^{4}He [16].

When dense helium is subjected to ionizing radiation, a complex set of reactions involving He_2^+, He_3^+ and metastable atoms and excimers become important [17]. The lifetimes of these metastable species are mostly dependent on two-body collisions involving excited species for both bodies. An interesting fact is that the lowest excimer state, the $a\,^3\Sigma_u^+$, calculated to have a long lifetime in vacuum, is metastable in the dense medium with a lifetime in excess of 10 s [18].

Our cryostat does not permit us to work below the λ point. The consequence is that macroscopic helium gas bubbles are present in the liquid and these are sensitive to the temperature and pressure of the sample. We shall present spectra taken from just irradiated liquid helium as well as spectra taken when a small amount of solid hydrogen is present in the bottom of the cell. For some of these, we shall be able to compare to spectra taken by us in just dense helium gas [19]. We shall demonstrate that the occurrence of molecular hydrogen spectra is a consequence of the solubility of the hydrogen in the liquid helium, which is strongly temperature dependent below 4.2 K. The width and shifts of the H_2 spectral lines will also be discussed and compared to those for excited atomic and molecular helium measured by others.

II. EXPERIMENT

Our experimental arrangement is not so different from that described in Refs. [19,2]. The accelerator is the 3 MV

Van de Graaff at the University of Guelph producing 3 MeV protons with a current density of ~ 20 nA/cm^2. (For one spectrum, as mentioned in the caption, 4 MeV protons were used at McMaster University.) The copper sample cell has the shape of a cube, with interior volume about 0.5 cm^3, on the tip of a Janis transfer line cryostat. The proton beam enters through a 15 μm thick nickel foil (which has been moved closer to the center of the cell from our previous experiments) that is clearly visible through the two quartz windows on the perpendicular faces of the cell. The sample cell is surrounded by an aluminum radiation shield with three holes at right angles to each other. All of this is contained by a vacuum shroud with room-temperature windows also made of synthetic quartz. One can look right through the cell at right angles to the proton beam. This optical configuration has been used by us for both absorption and emission experiments but this paper is reporting exclusively emission experiments.

On one side of the cell is a 0.3 m McPherson grating monochromator with either a 1200 line/mm holographic or a 600 line/mm grating, the latter blazed at 1 μm. It is configured with a Hamamatsu R3310 cooled phototube, sensitive from 0.36 to 1.0 μm, and standard photon counting electronics. A spherical and two plane mirrors image the entrance slit of the monochromator just behind the nickel foil of the cell, thereby collecting light emitted from a locally small region. This adjustment is made under operating conditions, i.e., with the cell full of liquid helium and the proton beam on. The one, and perhaps only, advantage to using a lower energy accelerator is that the radiation levels are sufficiently low that we can be physically present in the target room when the proton beam is on, allowing us to make the adjustment mentioned above.

On the opposite side of the shroud from the grating monochromator is a Bomem 157 Fourier Transform Spectrometer using a single CaF_2, 75 mm focal length lens as collimator. This instrument, having a 2 cm^{-1} spectral resolution, has been configured for low-light-level emission experiments and for the work reported here was using a cooled, InGaAs detector sensitive from 0.8 to 1.6 μm.

To achieve temperatures below 4.2 K, the exhaust of the transfer line can be pumped by a large rotary pump. The lowest stable temperature attainable within the cell using this system is 2.6 K. The cell temperature has been calibrated below 4.2 K by measuring the equilibrium vapor pressure of helium in the sample cell. The temperature inside the sample while the proton beam is on will be not more than 0.5 K higher than our quoted values.

III. RESULTS

A. Liquid-helium spectra

Before presenting spectra of hydrogen in liquid helium it is worthwhile looking at some spectra from the liquid itself. Figure 1 is representative of all of the spectral regions that we have studied that span 400–1600 nm. We have chosen to display the $D\,^1\Sigma_u^+ \rightarrow C\,^1\Sigma_g^+(0-0)$ near 7600 cm^{-1} taken with the Bomem spectrometer. At 2.8 K the vapor pressure of helium is 133 torr, which represents the lowest external

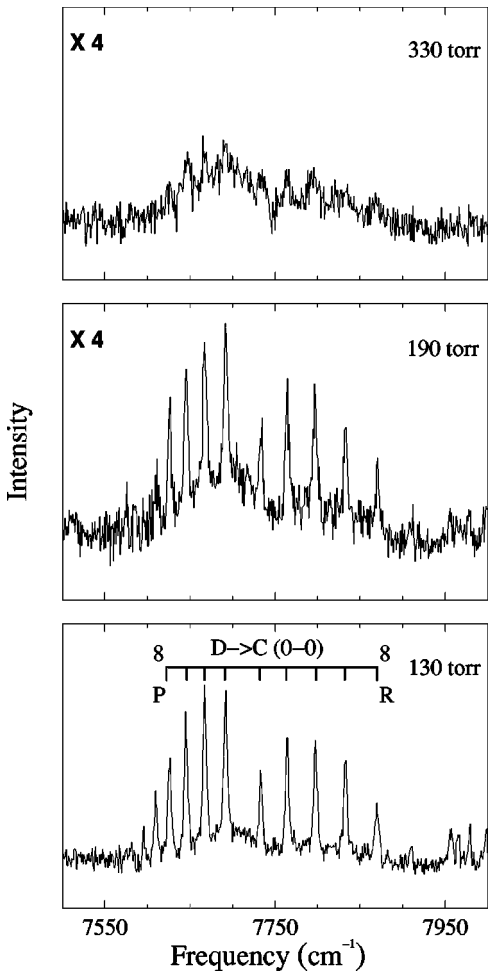

FIG. 1. The He_2 $D \rightarrow C(0\text{-}0)$ FTIR emission band for different pressures above the liquid at 2.8 K.

pressure that we could apply. Close to this limit we observe spectra with the most intense lines. As the external pressure is increased, the line intensity decreases until, at about 330 torr, the lines are essentially gone, leaving only a broad underlying background that we attribute to the liquid itself. Such broad, unresolved spectra have been observed by others in liquid helium below the λ point [20]. We attribute the line spectra as coming from macroscopic gas bubbles caused by local heating by the proton beam. A modest increase in the external pressure prevents these bubbles from forming. This result is independent of the wavelength being observed.

We have acquired gas phase spectra over a sufficient number of pressures to allow us to calibrate the linewidth as a function of gas pressure for a number of transitions of both the excimer He_2 and atomic He. An example of the gas spectrum can be seen in our previous work [19]. Such calibration allows us to conclude that the gas bubbles in the liquid have an internal pressure of 134(8) torr. If we use only the surface tension of liquid helium and elementary physics, this pressure converts to a bubble radius of 3 μm but the uncertainties in our pressures are greater than the pressure difference between the interior of the bubble and the bulk liquid, so we may conclude only that the bubble is larger than 0.3 μm. We have no way of precisely measuring the lifetime of these

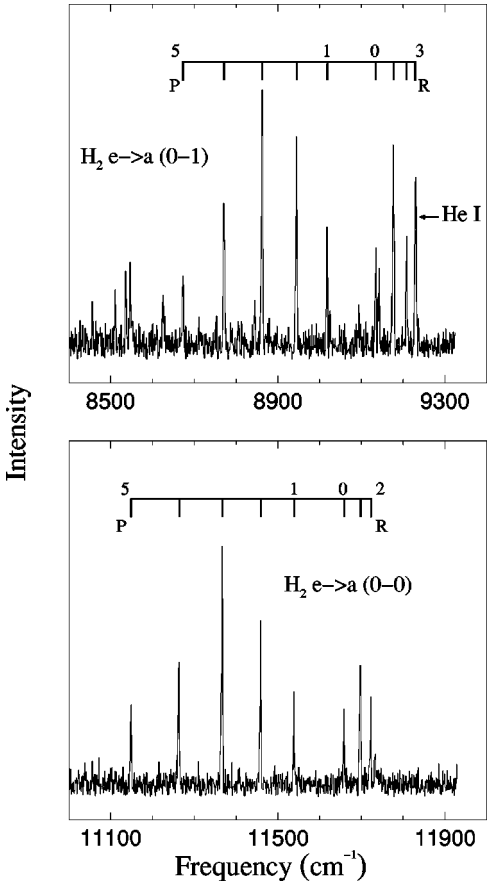

FIG. 2. The H_2 $e \rightarrow a(0\text{-}0)$ and $(0\text{-}1)$ FTIR emission bands for a sample of hydrogen-doped helium gas taken using 4.0 MeV protons. The gas temperature is 6 K and the pressure is 150 torr. The $R3$ line is blended with a He I line.

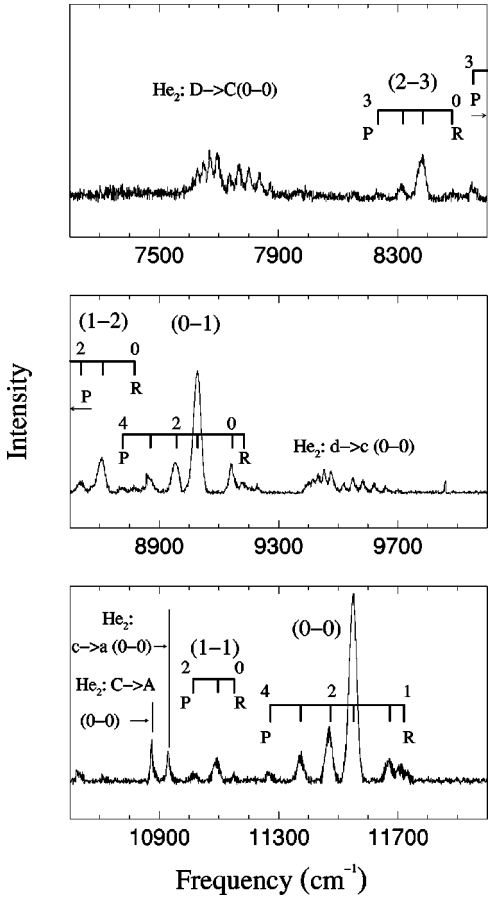

FIG. 3. FTIR survey spectrum of liquid helium above a film of solid hydrogen at 3.9 K and 650 torr. All rotationally identified transitions are of H_2. Intensities have been corrected for detector response.

bubbles, but can estimate that it is of the order of ms. This estimate is based on pulsed proton-beam absorption measurements, using a technique described previously [21]. We have observed an intense absorption signal, which was wavelength independent, that we attribute to light scattering from these macroscopic bubbles. This interpretation is reasonable because the technique is such that as little as a 0.1% decrease in lamp flux from Mie scattering would produce an intense signal. The bubbles would have to have a lifetime of the order of ms to be detected in such an experiment.

B. Hydrogen-doped gaseous helium

For comparison to spectra to be presented subsequently, and for their own sake, we present in Fig. 2 emission spectra of molecular hydrogen taken at 6 K in a sample of 150 torr helium gas using 4 MeV protons at McMaster. The intensities have been corrected for detector response. No energy dependence, other than emission line intensities, has ever been observed in our experiments. The conditions are identical to those that produce helium hydride emission [4] but no such emission was observed in the spectral regions under examination for this study. The partial pressure of hydrogen at 6 K is $(8\pm1)\times10^{-4}$ torr [22], and 150 torr of helium at 6 K optimizes the intensity of the hydrogen emission. That is consistent with what was observed for helium hydride. This observation that emission spectra are extremely sensitive to temperature and pressure conditions seems to hold generally for hydrogen-doped helium samples at these low temperatures. We have tried to observe hydrogen or helium hydride spectral features at warmer temperatures without success. Even pure hydrogen gas does not emit radiation that we can observe under any pressure or temperature conditions that we have tried, save the lowest pressures at which we have observed weak atomic emission lines.

All H_2 emission features that we are reporting arise from the e-a transition of the triplet state molecule. The two bands shown in the figure are the (0-0) in the lower panel and the (0-1) in the upper. Note that the $P(3)$ and $R(1)$ lines are the most intense, meaning that the $J=2$ rotational level of the upper state is preferentially populated. This converts to a rotational temperature of 480 K. The linewidths of 2 cm^{-1} are instrumental.

C. Hydrogen-doped liquid helium

Figure 3 shows a survey spectrum taken with the FTIR of a sample of liquid helium above a film of solid hydrogen at 3.9 K and 650 torr. (The spectral intensities in this figure and in Figs. 2 and 4 have been corrected for detector response; all

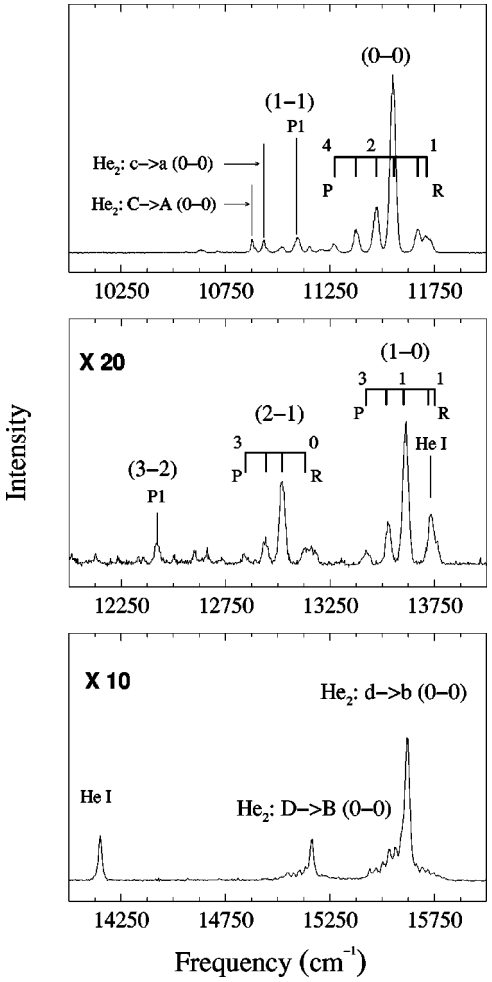

FIG. 4. Survey spectrum of liquid helium above a film of solid hydrogen at 3.9 K and 650 torr, recorded using the grating spectrometer. Identifications as in Fig 3. Intensities have been corrected for detector response.

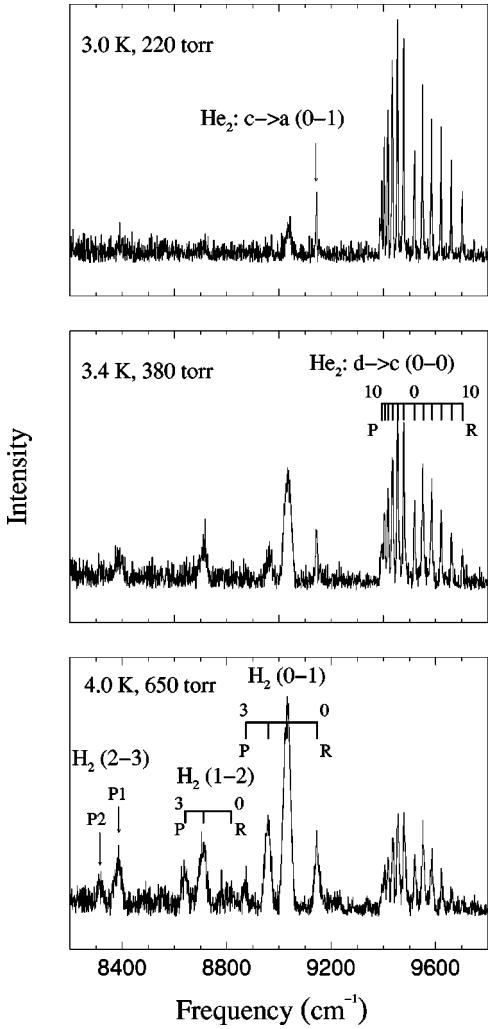

FIG. 5. Spectra recorded using the FTIR for three different temperatures of a sample of liquid helium above a film of solid hydrogen. The pressures are approximately the vapor pressures for the corresponding temperatures.

other figures are uncorrected intensities.) In contrast to the gas phase helium spectrum shown above, the liquid shows a more intense hydrogen spectrum with several vibrational bands, the most intense of which are the H_2 (0-0) and (0-1). Figure 4, taken with the grating spectrometer, covers the spectral region below 1 μm for the same sample conditions as the previous figure. Note that for every band, the strongest line is the $P(1)$, meaning that $J=0$ of the upper state is preferentially populated. The rotational temperature for H_2 in the liquid is about 35 K. Whether this is a consequence of inhibition of rotation of the molecule in the liquid or significantly different excitation conditions from the gas is not clear but we shall return to this question below.

The strongest emission spectrum is from the H_2 (0-0) band near 11 600 cm^{-1}. This band appears among the spectra from both spectrometers but has better signal-to-noise ratio using the PMT/grating combination than the FTIR. This is a consequence of the wavelength being close to the high frequency limit of the FTIR detector. Note that it appears much stronger than the He_2 emission bands near 15 500 cm^{-1} even though these bands are the strongest emission features from samples of pure helium. (It appeared three times stronger in the raw spectrum before correcting for detector response.) The presence of hydrogen quenches the helium transitions and we have observed that this is a general trend occurring for all helium emission features that we have studied. That the formation of helium hydride proceeds through interactions involving excited He_2 thereby quenching emission from that excimer, is a reasonable but not certain explanation for what is occurring. HeH could be present in the liquid, in the lowest electronic potential curve, and show no spectrum.

The intensity of the hydrogen features is a sensitive function of the temperature, as shown in Fig. 5. Each of these spectra were taken close to the vapor pressure of liquid helium for that temperature. Clearly the maximum hydrogen line intensity occurs at the highest possible temperature. Given our temperature uncertainties and our reluctance to rupture the seals of our sample cell, we did not try to work at 4.2 K but kept the temperature a few tenths lower than 4.2 K. The role that hydrogen plays in reducing the intensity of He_2 emission is clearly demonstrated in this figure as well.

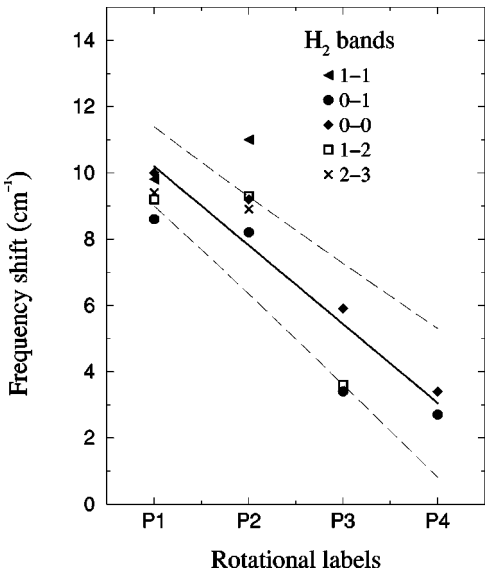

FIG. 6. Progression of the line shifts of the hydrogen emission features. The numbers in the rotational labels refer to the rotational quantum numbers of the lower electronic state.

The amount of hydrogen dissolved in the liquid helium at these temperatures is a matter of solubility and we are not aware of the relevant parameters being tabulated. Constructing an estimate, based on the gas phase vapor pressure of hydrogen at these temperatures, does not explain the gross temperature dependence. Using Eq. 4.5 from Ref. [22], we note that the vapor pressure of H_2 at 3.0 K is 5.7×10^{-11} torr while at 4.0 K it is 2.0×10^{-7} torr. If the concentration of H_2 really did decrease over three orders of magnitude in going from 4 K to 3 K, one would not be able to see any features at the lower temperature. Hence, obtaining concentration estimates from the gas phase does not appear useful and a more serious calculation would have to be performed to explain the observed spectral intensities.

IV. DISCUSSION

The most notable feature of the spectra of H_2 in liquid helium is that the lines are broader than those of He_2 and much broader than the same lines taken in the gas phase. When one remembers that we attribute the He_2 lines to emission from macroscopic gas bubbles and have argued that emission from the liquid itself underlies the line spectrum and is quite broad, it might then be considered unusual that any H_2 lines were observed at all. Besides being broadened, the lines are blue shifted, that is, the centroids of the lines have been shifted to higher frequencies.

The *P*-branch line positions of the hydrogen bands were compared to the transition energies calculated from the energy levels given in Ref. [23]. The features are all blue shifted between 2 and 11 cm^{-1} and there is a progression in the magnitude of the line shift as is indicated by Fig. 6. All of the hydrogen features are broadened to between 30 and 35 cm^{-1}, which lies beyond the linewidth of the FTIR and the grating monochromator (2 and 5 cm^{-1}, respectively). The widths and shifts of the emission lines do not appear to vary much with temperature, as can be seen from the spectra presented in Fig. 5.

The existence of a bubble surrounding an excited atom in liquid helium was first suggested by Dennis *et al.* [8] and has since been confirmed by several groups working on excited atoms [13,24–26]. A cavity in the liquid helium is formed because of repulsive forces between the excited atom and the surrounding helium atoms. Free electrons in liquid helium are known to form such bubbles and their infrared spectrum has been observed (see [27,28] and references therein). In view of this body of work it is reasonable to attribute the small shifts observed in our work to cavities formed around the excited molecules. Indeed, the H_2 molecule in its excited state ($e\,^3\Sigma_u^+$) is too large to fit inbetween the He atoms in the liquid. Calculations based on the model presented indicated that the average radius of the valence electron is about 8 Å , while the average He-He separation based on the bulk density is about 3.5 Å . The size of the cavity formed in liquid helium by an excited molecule and the effect of this cavity on the line position is evaluated following the method of Hickman *et al.* [24]. A brief outline of this calculation follows.

A. Model calculation: line shift

The helium atoms surrounding the cavity are assumed to follow a density profile first introduced by Hiroike *et al.* [12]. Apart from the bulk density of the liquid helium, only two parameters are needed to describe the density profile for a spherical cavity: the zero-density radius (R_0) and the width (α^{-1}) of the transition region. An additional term, can be used to describe deviations from spherical symmetry. The exact form of the density profile in its spherical and nonspherical form can be found in previous publications [12,13,24].

The size of the cavity is governed by the interaction between the excited molecule and the surrounding He atoms. The cavity size will remain constant on the time scale of a transition. Thus for both emission and absorption, the cavity geometry is always determined by the initial state of the transition. This explains why the magnitude and sign of the line shift can differ between absorption and emission experiments [13,20].

The He-He interaction energy in the liquid is assumed to be the same in both the upper and lower electronic states of the molecule. This energy does not contribute to the line shift and is set to zero for convenience. The energy of the system is then (using atomic units)

$$E_{\text{total}}=E_{\text{excited}}+4\pi R_b^2\gamma+\frac{4}{3}\pi R_b^3 p, \tag{1}$$

where E_{excited} is the energy of the excited molecule in the cavity, γ is the surface tension, and p is the pressure of the liquid. R_b is the effective radius of the cavity, given approximately by $R_b\sim R_0+2\alpha^{-1}$. A volume kinetic energy term has been neglected in favor of using the experimental value of the surface tension (γ) of liquid He at 4 K.

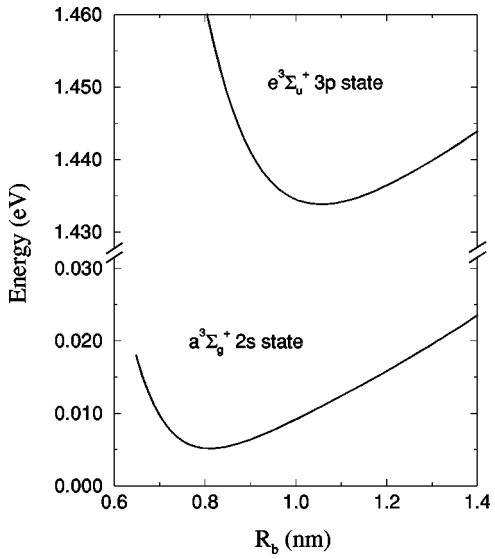

FIG. 7. Total energy of the cavity formed by an excited hydrogen molecule in liquid helium as a function of the radius of the cavity. The upper curve refers to the initial state of the emission features.

The difficulty lies in evaluating E_{excited} because this demands knowledge of the interaction potential between a ground-state He atom and an electronically excited H_2 molecule. At this time, this potential is not known. It is at this stage that our calculation departs to some extent from the calculation of [24], where the energies are evaluated by first order perturbation theory.

The model consists of an excited molecule at the center of a spherical cavity in the liquid He. We assume that the molecule can be described by an H_2^+ core and a valence electron. The screening due to the inner electron is represented by a δ-function potential shell of radius ~ 0.5 Å. The amplitude of the pseudopotential is chosen so that the calculated energy of the valence electron corresponds to the unperturbed electronic energy of the excited state.

The energy terms used to evaluate E_{excited} include the same electron-helium pseudopotential introduced in [24] as well as a standard Van der Waals term. The interaction of the H_2^+ core and the He atoms of the liquid is neglected. We solve the radial Schrödinger equation of the valence electron in the cavity, thus obtaining E_{excited} and the perturbed wave function of the valence electron.

This calculation is performed for different cavity sizes when the molecule is in the upper electronic state ($e\ ^3\Sigma_u^+$). The cavity size, which minimizes the total energy of the system, is taken as the average size of the cavities formed by the excited molecule. The calculations are then repeated for the lower electronic state ($a\ ^3\Sigma_g^+$) and the energy difference at the average cavity size, obtained previously, yields the perturbed transition energy.

The calculation was performed for a single cavity in a sample of bulk liquid He at 4 K. The energy of the system for both excited states is plotted in Fig. 7, where the zero of potential energy is taken as the sum of the He-He interaction energy from the bulk liquid and the unperturbed energy of the $a\ ^3\Sigma_g^+$ state. From the minimum of the upper state curve, we calculate that the average cavity radius is $R_b \sim 1.06$ nm. A free electron forms a cavity in the liquid with a radius lying between 1.2 and 1.4 nm [9,12]. For the case of excited He atoms in liquid He, Hickman *et al.* [24] calculates the radius of the cavity formed by a He atom in the $3\ ^3S$ and $3\ ^1S$ states to be 1.11 nm and 1.30 nm, respectively. Kinoshita *et al.* calculate the radius to be 0.735 nm for excited Cs atoms in liquid He at 1.6 K [26].

TABLE I. Table of the H_2: $e\ ^3\Sigma_u^+ \rightarrow a\ ^3\Sigma_g^+$ lines in the 4.0 K, 650 torr liquid He spectrum above solid hydrogen. All entries are in cm^{-1}. Uncertainties in parentheses are 1 standard deviation.

Band	Line	Liquid	FWHM	Gas phase[a]	Difference
2-3	$P2$	8311.6(1.0)	33(4)	8302.71	8.9(1.0)
	$P1$	8379.1(0.4)	34(1)	8369.69	9.4(0.4)
1-2	$P3$	8550.0(1.0)	34(4)	8546.36	3.6(1.0)
	$P2$	8634.8(0.8)	30(3)	8625.47	9.3(0.8)
	$P1$	8704.6(0.8)	30(2)	8695.45	9.2(0.8)
0-1	$P4$	8774.0(2.0)	22(3)	8771.29	2.7(2.0)
	$P3$	8865.6(1.0)	24(5)	8862.20	3.4(1.0)
	$P2$	8952.9(0.2)	29(1)	8944.67	8.2(0.2)
	$P1$	9026.5(0.2)	29(1)	9017.87	8.6(0.2)
1-1	$P2$	11015.3(1.0)	33(13)	11004.30	11.0(1.0)
	$P1$	11090.4(0.6)	31(5)	11080.57	9.8(0.6)
0-0	$P4$	11266.4(0.4)	21(5)	11263.31	3.1(0.4)
	$P3$	11373.0(0.3)	24(4)	11367.06	5.9(0.3)
	$P2$	11468.4(0.3)	27(2)	11459.23	9.2(0.3)
	$P1$	11548.9(0.3)	30(1)	11538.94	10.0(0.3)

[a]Reference [23]

Using the curves presented in Fig. 7, we find that the effective energy shift is $+16.7\ \text{cm}^{-1}$. This should be compared to the shifts tabulated in Table I. As can be seen our results are within a factor of 2 of the average of the energy shifts reported. Kinoshita *et al.* report an energy shift of $27.7\ \text{cm}^{-1}$ for excited Cs atoms [26], while Hickman *et al.* [24] report an energy shift of $\sim 40\ \text{cm}^{-1}$ for the He $2\ ^3P$-$3\ ^3S$ emission line. Our calculation cannot account for the progression of the line shift with changing rotational state (see Fig. 6) since it treats the excited molecule with spherical symmetry.

B. Model calculation: linewidth

As has been mentioned previously, the hydrogen emission features are broadened to about $\sim 30\ \text{cm}^{-1}$. Two methods were used to evaluate the line shape of the emission lines. The first is based on standard line-broadening theory and we use the same method outlined in Sec. IV of Ref. [24]. The critical term in these expressions is $\Delta V(R)$, the difference in the interaction potential energies in the upper and lower electronic states. In our calculation, $V(R)$ is taken to be

$$V(R) = -\frac{\alpha_{\text{He}}}{R^6}\langle r^2\rangle + \int d^3\vec{r}\,[u_{\ell}(r)]^2 V_{\text{ps}}(|\vec{R}-\vec{r}|) \quad (2)$$

where $\vec{R}$ and $\vec{r}$ are the positions of the helium atom and the

electron, respectively. The first term is a standard Van der Waals attractive term with α_{He} the polarizability of ground-state He. The second term represents the interaction between the valence electron and the He atoms of the liquid. $u_l(r)$ is the radial wave function of the electron, calculated for the average cavity size and $V_{\mathrm{ps}}(|\vec{R}-\vec{r}|)$ is the same e-He pseudopotential used in our calculations of the cavity size and line shift. The linewidth resulting from this calculation is too large by a factor of 4 and the associated line shift too large by a factor of 20.

The second method uses the cavity energy curves shown in Fig. 7, treating them as potential energy curves describing the breathing mode of the cavity. The cavity formed by the molecule in its upper excited state is assumed to be in thermal equilibrium with the liquid. Thus at 4 K there is a thermal energy associated with the breathing mode of the cavity. If one considers the ensemble of cavities in the bulk liquid, then at the instant a transition occurs there should be a distribution of possible cavity sizes. An effective line shift ω can be calculated for each cavity size from the difference of the cavity energy curves.

The line shape is constructed by plotting the probability that a given line shift will occur, $P(\omega)$, as a function of that shift. $P(\omega)$ is governed by the Boltzmann distribution of cavity sizes

$$P(\omega)d\omega = e^{-\beta \Delta E(R_b)} dR_b, \tag{3}$$

where R_b is the effective cavity radius, $\Delta E(R_b)$ is the energy difference between the cavity energy and the minimum cavity energy in the initial state, and $\beta = 1/k_B T$ at 4 K. The reader is reminded that the energy curves plotted in Fig. 7 represent the electronic energy of the molecule in the given electronic states. Thus the transition energy obtained from the difference of both curves for some value of R_b represents the sum of the unperturbed electronic transition energy ($T_0 \sim 1.42$ eV) and the induced energy shift (ω).

The results are displayed in Fig. 8. In order to compare the resulting line shape with experimental data, ω was shifted by $+9017.12$ cm^{-1}, the unperturbed transition energy of the e-a (0-1) $P1$ emission line. This feature is the strongest hydrogen line in the spectrum shown in Fig. 3. As can be seen, the centroid of the calculated line shape lies about 7 cm^{-1} to the right of the experimental line center. In addition, the FWHM of the calculated line is only ~ 20 cm^{-1} compared to the 30 cm^{-1} of the observed emission line.

The centroid of the calculated line profile is determined by the energy difference between the energy curves of Fig. 7 at the equilibrium cavity size. The width and symmetry of the profile depend on the actual curvature of the energy curves. These are calculated from the energy expression of Eq. (1), which, for small values of R_b, is dominated by the energy of the excited molecule in the cavity E_{excited}. Thus closer agreement with experimental data may be achieved if the method for calculating E_{excited} can be improved.

We have shown in some detail two attempts to model the linewidth. The first, based on an extension of the standard line-broadening theory, resulted in a linewidth too broad by a factor of 4. The second method, based on a simpler statistical argument, yields a result that agrees much better with the observed linewidths. However, it is still in error by a full third of the observed width.

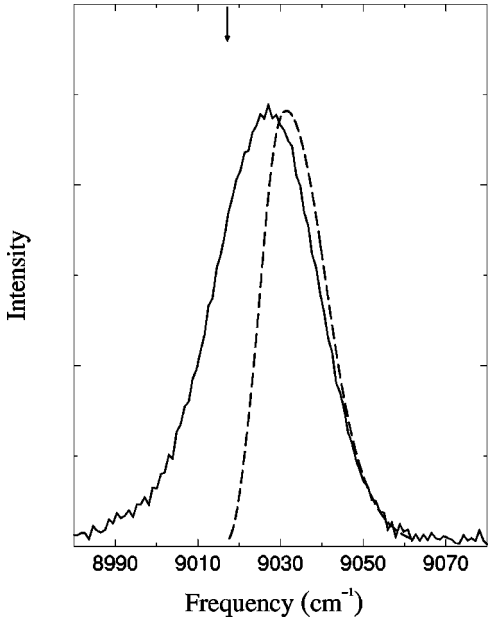

FIG. 8. The (0-1) $P1$ line of Fig. 3 (solid line) and the profile calculated using the method outlined in Sec. IV B (dashed line). The frequency of the unperturbed transition is marked by the arrow.

There is a third method, proposed in [26], that is similar to the second width calculation. The method involves treating the potential curves as potentials in a one-dimensional problem. The eigenfunctions are calculated from the Schrödinger equation and Frank-Condon-type arguments are applied. Application of this idea leads to a line shape whose centroid is unchanged, but whose width is ~ 6 cm^{-1}. Clearly there is more work to be done on this problem.

V. CONCLUSION

We have presented spectra of molecular hydrogen doped into a sample of liquid helium at temperatures above the λ point. An analysis of the spectral shifts and widths has been performed using a slight variation on work done previously with only modest success. The shifts were predicted to be too large by nearly a factor of 2 and the widths too narrow by about the same factor. That the spectral shifts of the lines showed a decrease with increasing rotational quantum number has not been explained. Even if the model presented were modified to account for nonspherical symmetry, one would have to incorporate a coupling between the electron and nuclear motions. Such couplings, accounting for one type of Born-Oppenheimer breakdown, would present a significant complication to the model presented here.

Another feature, clearly seen in the spectra but not explained, may also be related to a coupling of electronic and

nuclear motion; that is, the change in the distribution of rotational intensities observed in the doped liquid spectra as compared to the doped gaseous spectra. We recorded a drop in rotational temperature from 480 K to 35 K in going to the liquid. While this may be related to the much slower proton-beam velocity in the liquid, in fact we have never observed a change in rotational intensities in gas phase spectra when the beam energy was changed.

The study of molecular spectra from a liquid-helium host offers insights and challenges different from but complementary to the study of doped atoms.

ACKNOWLEDGMENTS

We are grateful for support from the Natural Sciences and Engineering Research Council (NSERC) of Canada, and we wish to thank Bill Teesdale and Tom Riddols for technical help. Special thanks are extended to B. G. Nickel for helpful suggestions regarding the calculations.

[1] J. Peter Toennies and Andrei F. Vilesov, Annu. Rev. Phys. Chem. **49**, 1 (1998).
[2] R.L. Brooks and J.L. Hunt, J. Chem. Phys. **88**, 7267 (1988).
[3] R.L. Brooks, J.L. Hunt, and J.J. Miller, Phys. Rev. Lett. **58**, 199 (1987).
[4] R.L. Brooks and J.L. Hunt, J. Chem. Phys. **89**, 7077 (1988).
[5] C.M. Surko and F. Reif, Phys. Rev. **175**, 229 (1968).
[6] M.R. Fishbach, H.A. Roberts, and F.L. Hereford, Phys. Rev. Lett. **23**, 462 (1969).
[7] The temperature at which liquid helium becomes superfluid ~ 2.18 K for ^{4}He.
[8] W.S. Dennis, E. Durbin, Jr., W.A. Fitzsimmons, O. Heybey, and G.K. Walters, Phys. Rev. Lett. **23**, 1083 (1969).
[9] B.E. Springett, M.H. Cohen, and J. Jortner, Phys. Rev. **159**, 183 (1967).
[10] W.B. Fowler and D.L. Dexter, Phys. Rev. **176**, 337 (1968).
[11] J. Jortner, N.R. Kestner, S.A. Rice, and M.H. Cohen, J. Chem. Phys. **43**, 2614 (1965).
[12] K. Hiroike, N.R. Kestner, S.A. Rice, and J. Jortner, J. Chem. Phys. **43**, 2625 (1965).
[13] S.I. Kanorsky, M. Arndt, R. Dziewior, A. Weis, and T.W. Hänsch, Phys. Rev. B **50**, 6296 (1994).
[14] Y. Takahashi, K. Sano, T. Kinoshita, and T. Yabuzaki, Phys. Rev. Lett. **71**, 1035 (1993).
[15] B. Tabbert *et al.*, Z. Phys. B: Condens. Matter **97**, 425 (1995).
[16] B. Tabbert, H. Günther, and G. zu Putlitz, J. Low Temp. Phys. **109**, 653 (1997).
[17] D.W. Tokaryk, R.L. Brooks, and J.L. Hunt, Phys. Rev. A **48**, 364 (1993).
[18] D.N. McKinsey, C.R. Brome, J.S. Butterworth, S.N. Dzhosyuk, P.R. Huffman, C.E.H. Mattoni, J.M. Doyle, R. Golub, and K. Habicht, Phys. Rev. A **59**, 200 (1999).
[19] D.W. Tokaryk, G.R. Wagner, R.L. Brooks, and J.L. Hunt, J. Chem. Phys. **103**, 10 439 (1995).
[20] W. A. Fitzsimmons, *Atomic Physics 3* (Plenum, New York, 1973), pp. 477–492.
[21] R.L. Brooks, J.L. Hunt, and D.W. Tokaryk, J. Chem. Phys. **91**, 7408 (1989).
[22] P. C. Souers, *Hydrogen Properties for Fusion Energy* (University of California Press, Berkeley, 1986).
[23] H. M. Crosswhite, *The Hydrogen Molecule Wavelength Tables of Gerhard Heinrich Dieke* (Wiley, New York, 1968).
[24] A.P. Hickman, W. Streets, and N.F. Lane, Phys. Rev. B **12**, 3705 (1975).
[25] H. Bauer *et al.*, Phys. Lett. A **146**, 134 (1990).
[26] T. Kinoshita, K. Fukuda, Y. Takahashi, and T. Yabuzaki, Phys. Rev. A **52**, 2707 (1995).
[27] C.C. Grimes and G. Adams, Phys. Rev. B **45**, 2305 (1992).
[28] M. Rosenblitz and J. Jortner, Phys. Rev. Lett. **75**, 4079 (1995).